INFRARED PHOTOMETRIC STUDY OF FIELD POPULATION II STARS

LEE, SANG-GAK

Department of Astronomy, Seoul National University, Seoul, Korea
E-mail : sanggak@astrosp.snu.ac.kr

BRUCE, W. CARNEY

Department of Physics and Astronomy, University of North Calorina, Chapl Hill, NC27514, USA
E-mail : bruce@envy.astro.unc.edu

ROBERT, PROBST

Kitt Peak National Observatory, Tucson AZ USA
E-mail : probst@noao.edu

ABSTRACT

Near infrared JHK magnitudes are presented for two hundred two high proper motion stars. We have observed high proper motion stars in the near-infrared bands(JHK) using the COB detector on the Kitt Peak 1.3m, 2.1m and 4m telescopes. The observations and data reduction procedures are described. The infrared color magnitude diagram and color-color diagrams for the program stars are presented.

Key Words : JHK infrared photometry, LHS stars, high proper motion stars, population II stars

I. INTRODUCTION

Field population II stars have been known as the fossils of the early formation of the Galaxy. The luminosity function and mass function for these stars give important clues for early star formation history as well as basic informations of the local halo mass density. The first attempt to get the halo luminosity function from the local halo stars was done by Schmidt(1975) two decades ago. He used the Lowell Proper Motion Catalogue(Giclas et al. 1968) to get a complete sample of stars with proper motion larger than 1.295 seconds of arc per year. With a sample of 18 high proper motion stars, he estimated the local halo-to-disk mass ratio of 0.125%. Subsequent studies on this subject from the local halo stars were done by Eggen(1983, 1987), Dawson(1986), Lee(1985, 1991, 1993, 1995), Bahcall and Casertano(1986) and Dahn et al. (1995). However their results are not in good agreements, especially in the faint end of the lunimosity function, which part is the most important to give a clue whether halo low mass stars are enough for the dark matters or not. The slopes of the luminosity functions by Eggen(1983) and Bahcall and Casertano(1986) showed continuously increasing luminosity function with decreasing luminosities while recent work of Dahn et al. showed a turnover in the luminosity function at the faint end. The non-local halo luminosity function study by Richer and Fahlman(1992), however, is yielded a function which rises rapidly to lower luminosities. The corresponding mass function, if extended down to the vicinity of 0.01 m_o, can flatten the Galactic rotation curve.

The starcount study on the ground has been best fitted for model with the halo luminosity function which has an average globular cluster function to $M_v = 6.25$ and the near-by luminosity function at fainter magnitudes with a local number density normalization of 1/600 that of the disk(Reid and Majewski 1993). Recent deep pencil beam surveys of the Hubble Space Telescope by Bahcall et al. ,(1995), Elson et al. ,(1996), Medez et al. ,(1996) revealed that the observed halo stars are far less than the model prediction if an adopted halo luminosity function is increasing towards the faint magnitudes and concluded that halo faint stars are not sufficient for the dark matter.

However the theoretical work of mass-magnitude relation of low-mass stars by Kroupa and Tout(1997) argue that the peak in the stellar luminosity function at $M \sim 11.5(m \sim 0.35\ m_o)$ for population I stars results from the minimum in dm/dM_p and the peak position in the stellar luminosity function depends strongly on the metallicity.

This implies that we can not adopt a halo luminosity function by just scaling down the disk luminosity function.

Therefore the halo luminosity function derived from the directly observed stars is mostly needed to interpret the starcount data on the ground as well as that of the Hubble Space Telescope.

Since the main problem of the most local halo luminosity function studies is the small number statistics. To get a large sample of halo stars, we use the LHS catalogue of Luyten(1979). Since the high proper motion stars are either nearby disk stars or high velocity population II stars, the sample of halo star candidates are selected by the reduced proper motion diagram and JHK bands are used to get the intrinsically faint stars.

First result of JHK magnitudes for the halo candidate stars are presented in this paper and the continuous work on the JHK photometry for halo candidate stars and the analysis for the luminosity function and mass function for halo stars will be presented in the next paper.

Observations and data reduction are described in Section II. Photometric results are presented in Section III

II. OBSERVATIONS

(a) The Program Stars

The list of target halo stars was generated from the LHS proper-motion catalog of Luyten (1976). Program objects were chosen in the reduced proper motion diagram among the stars with color class of k and m of the LHS Catalogue. Because of the limited time of observation, target stars were restricted to the bright stars which r magnitudes in LHS are less than 18 and the stars located in north of $\delta > 0$ degree. Among them the stars located in the galactic latitude less than 10 degree were exculded because the LHS catalogue itself is not completed in these regions due to the crowdness of stars.

(b) Observations and Data Reduction

All observations were obtained using the Cryogenic Optical Bench (COB) at the Kitt Peak National Observatory. COB uses a 256 × 256 InSb array with 40 μm pixels. At near-infrared wavelengths (JHK), the detector quantum efficiency exceeds 90%, with a well depth of 200,000 electrons. COB was used on three different telescopes, yielding three different image scales: 0.93″/pixel at the 1.3-meter, 0.5″/pixel at the 2.1-meter, and 0.3″/pixel at the 4-meter. The gain was set to 6.6 electrons per ADU so that the well depth would match the 16-bit system limit of 32761 ADU. However, the detector begins to display non-linearities at the highest count levels, and care was thus taken to limit the peak counts to ≤ 5000 ADU in almost all cases, and in no case more than 10000 ADU. The detector dark current was less than 1 electron/sec/pixel, and the read noise was 35 electrons/pixel per read. Most observations were obtained using the multiple read option, with N = 8, with consequent reduction in read noise, but a fainter limit to the brightest stars that could be observed.

Table 1.   Journal of Observations for Field Population II stars.

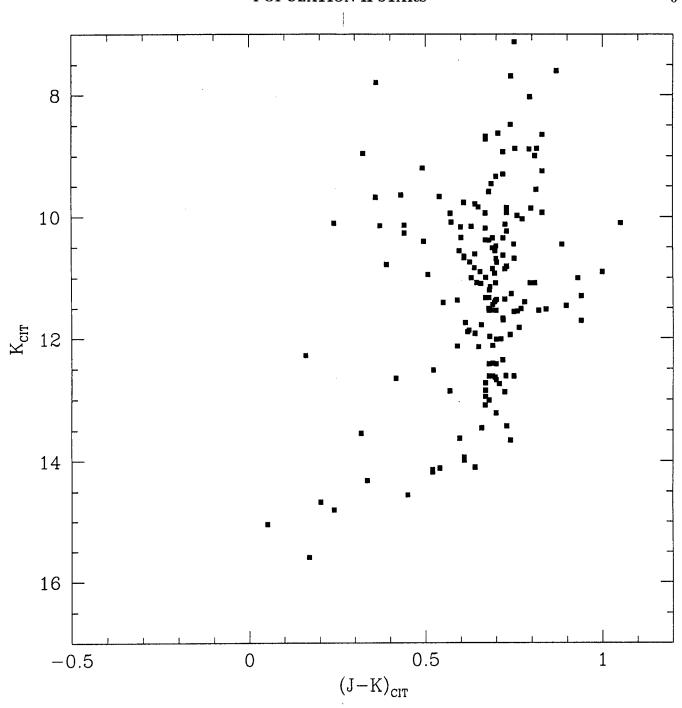| Date(UT)	IR Detector	Telescope	Image Scale(/pixel)
Dec 19 - 22 1994	COB	1.3m	0.93 /pixel
May 12 - 19 1995	COB	2.1m	0.50 /pixel
Jun 10 - 14 1995	COB	4.0m	0.30 /pixel

Fig. 1. Infrared K versus $(J - K)$ Color-Magnitude Diagram for the Program Stars

The observing procedures during each run were the same. During the afternoons long sequences of "dark" frames would be taken with the cold stop in position. The frames were taken with all exposure times anticipated during the night since the dark current appears to have some non-linear behavior. The multiple dark frames were median filtered and combined into single images, each with a different exposure time.

The photometric observations were carried out only during half or full nights of completely cloudless skies. Standard star and program stars were observed multiple times, with the telescope being moved between each exposure, so that the images would appear in a pre-determined sequence of locations on the detector array. The multiple observations served three purposes: improved photon statistics, especially for the fainter program stars;
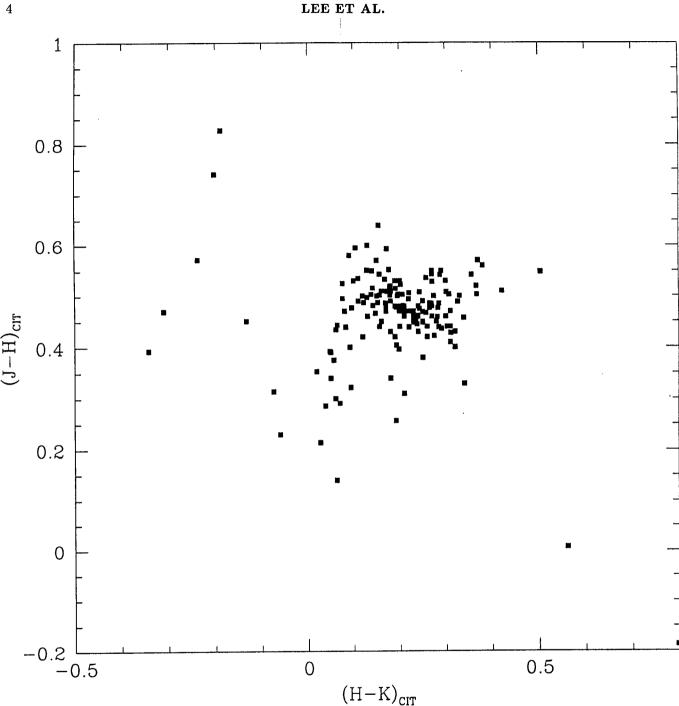
Fig. 2. Infrared $(J - H)$ versus $(H - K)$ Color-Color Diagram for the Program Stars

sampling over a wider area of the detector, reducing possible systematic effects from residual problems in flatfielding; and the steady production of high-quality flatfield exposures, which could be obtained by median filtering the multiple program star observations. For most but not all of the nights, there was no change in the flatfields, but in a few cases, there was a slow evolution in the detector sensitivity, and having flatfields obtained throughout the course of the night removed most of the effects.

All reductions of the observed image frames have been done by IRAF(Image Reduction and Analysis Facilities) routine. Instrumental magnitudes of the stars in the image frames were measured by using IRAF/DAOPHOT (Stetson 1987, 1990)
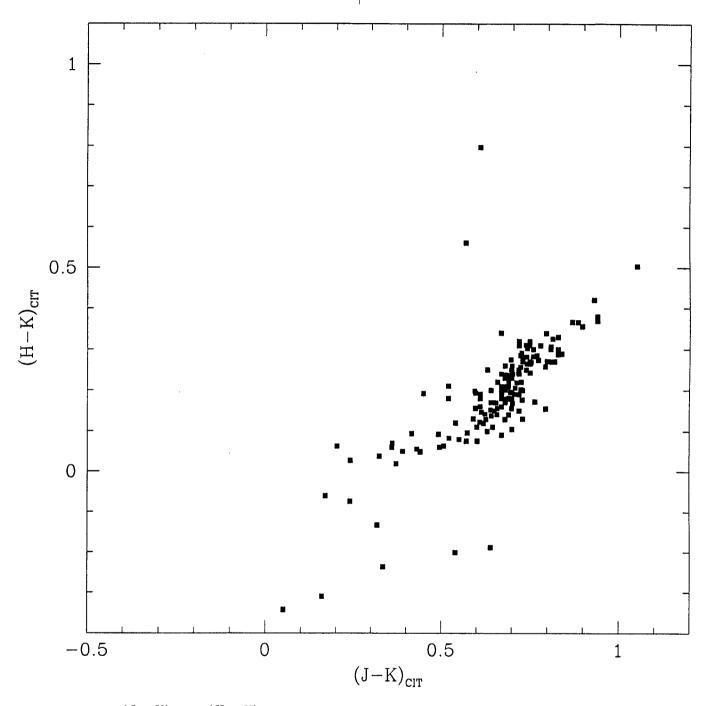
Fig. 3. Infrared $(J - K)$ versus $(H - K)$ Color-Color Diagram for the Program Stars

On every workable night, standard stars were observed. These were taken from the set of UKIRT standards (Casali & Hawarden 1992), which were designed for use with high quantum efficiency detectors working on large telescopes. Atmospheric extinction at J, H, and K was measured during each observing run, and found to be slightly variable. At K, for example, it varied from 0.05 mag/airmass during the driest period (December 1994) to 0.15 mag/airmass during the most humid observing run (June 1995). We found no evidence for a color term in the transformation from the "natural system" k magnitudes to the standard system K values, while the slopes of the color transformations to the standard system $J - K$, $J - H$, and $H - K$ values were constant (and roughly 1.07, 1.02, and 1.05, respectively). During the longer nights of December, 1994, 10 to 12 standards were observed per night,

LEE ET AL.

TABLE 2. JHK Photometry for the Program Stars.

	UKIRT System						CIT System			
Star	K	σ	$(J-K)$	$\sigma J-K$	$(H-K)$	$\sigma H-K$	K	$(J-K)$	$(H-K)$	ol
LHS42	8.642	0.016	0.755	0.017	0.199	0.019	8.629	0.706	0.191	D
LHS55	8.310	0.010	0.760	0.050			8.300	0.720		M
LHS103	9.474	0.013	0.734	0.015	0.245	0.013	9.461	0.687	0.235	D
LHS139	9.875	0.007	0.854	0.009	0.282	0.011	9.860	0.799	0.271	D
LHS140	9.013	0.008	0.865	0.011	0.320	0.009	8.997	0.810	0.307	D
LHS152	10.398	0.005	0.727	0.007	0.134	0.009	10.385	0.680	0.129	D
LHS211	10.116	0.010	1.124	0.010	0.525	0.012	10.096	1.052	0.504	D
LHS232	10.850	0.017	0.683	0.017	0.159	0.017	10.838	0.639	0.152	D
LHS239	14.680	0.060	0.217	0.065	0.066	0.105	14.676	0.203	0.063	D
LHS240	15.044	0.053	0.054	0.068	0.356	0.078	15.043	0.051	0.342	D
LHS279	10.573	0.010	0.745	0.012	0.286	0.012	10.559	0.697	0.275	D
LHS283	7.139	0.016	0.802	0.018	0.276	0.016	7.125	0.751	0.265	D
LHS296	8.892	0.011	0.806	0.016	0.280	0.012	8.878	0.754	0.269	D
LHS301	8.894	0.011	0.871	0.011	0.340	0.011	8.879	0.815	0.326	D
LHS307	11.523	0.009	0.726	0.016	0.241	0.013	11.510	0.679	0.231	D
LHS316	7.618	0.011	0.930	0.012	0.383	0.014	7.601	0.870	0.367	D
LHS320	9.960	0.010	0.710	0.010	0.220	0.000	9.940	0.670	0.210	M
LHS343	10.620	0.010	0.680	0.010	0.210	0.000	10.610	0.640	0.200	M
LHS345	9.860	0.010	0.780	0.010	0.290	0.000	9.850	0.730	0.280	M
LHS361	13.550	0.080					13.540			M
LHS370	10.250	0.020	0.780	0.020	0.290	0.000	10.240	0.730	0.280	M
LHS376	10.360	0.010	0.740	0.020	0.230	0.000	10.350	0.690	0.220	M
LHS399	8.090	0.000	0.800	0.000			8.070	0.750		M
LHS400	9.610	0.020	0.720	0.030	0.240	0.000	9.590	0.680	0.230	M
LHS403	8.940	0.010	0.770	0.010	0.330	0.000	8.930	0.720	0.320	M
LHS414	10.200	0.010	0.710	0.020	0.250	0.000	10.190	0.670	0.240	M
LHS425	11.020	0.020	0.680	0.020	0.270	0.000	11.000	0.630	0.250	M
LHS446	9.320	0.010	0.770	0.020	0.320	0.000	9.300	0.720	0.310	M
LHS453	13.950	0.050	0.650	0.050	0.200	0.000	13.940	0.610	0.190	M
LHS514	9.200	0.000	0.740	0.010			9.190	0.690		M
LHS522	10.860	0.010	0.730	0.020	0.150	0.000	10.850	0.690	0.140	M
LHS536	11.007	0.011	0.717	0.015	0.208	0.011	10.995	0.671	0.199	D
LHS1041	11.109	0.016	0.702	0.017	0.147	0.016	11.096	0.657	0.141	D
LHS1089	12.888	0.015	0.773	0.025	0.297	0.019	12.874	0.724	0.285	D
LHS1120	11.839	0.027	0.818	0.030	0.180	0.032	11.824	0.765	0.172	D
LHS1138	10.754	0.007	0.669	0.010	0.135	0.011	10.742	0.626	0.129	D
LHS1156	10.868	0.013	0.775	0.013	0.210	0.014	10.854	0.725	0.202	D
LHS1180	11.754	0.019	0.655	0.022	0.153	0.031	11.742	0.613	0.147	D
LHS1187	11.565	0.006	0.812	0.019	0.295	0.009	11.550	0.760	0.283	D
LHS1223	14.321	0.085	0.358	0.093	0.247	0.105	14.315	0.335	0.237	D
LHS1257	11.682	0.007	0.769	0.011	0.261	0.011	11.669	0.719	0.250	D
LHS1319	11.459	0.009	0.737	0.016	1 0.188	0.012	11.446	0.690	0.181	D
LHS1368	10.414	0.009	0.529	0.013	0.063	0.010	10.404	0.495	0.061	D
LHS1403	11.375	0.008	0.749	0.010	0.175	0.009	11.362	0.701	0.168	D
LHS1410	11.934	0.012	0.684	0.020	0.196	0.012	11.922	0.640	0.188	D
LHS1420	12.027	0.026	0.761	0.031	0.228	0.032	12.013	0.713	0.219	D
LHS1425	11.281	0.011	0.794	0.014	0.315	0.011	11.267	0.743	0.303	D
LHS1429	10.957	0.014	0.542	0.018	0.067	0.015	10.947	0.507	0.064	D

TABLE 2. (continued)

Star	UKIRT System						CIT System		
	K	σ	$(J-K)$	$\sigma J-K)$	$(H-K)$	$\sigma H-K)$	K	$(J-K)$	$(H-K)$
LHS1786	9.355	0.010	0.748	0.010	0.110	0.010	9.342	0.700	0.105
LHS1788	10.939	0.011	0.744	0.016	0.247	0.014	10.925	0.696	0.237
LHS1889	14.812	0.164	0.256	0.169	0.077	0.173	14.807	0.240	0.074
LHS1906A	11.554	0.007	0.726	0.009	0.186	0.011	11.541	0.680	0.179
LHS1913A	9.571	0.009	0.868	0.010	0.281	0.009	9.556	0.813	0.270
LHS1923	11.100	0.011	0.851	0.017	0.353	0.014	11.085	0.796	0.339
LHS1946	10.146	0.011	0.470	0.013	0.050	0.011	10.138	0.440	0.048
LHS1947	10.353	0.010	0.642	0.012	0.079	0.011	10.341	0.601	0.076
LHS1954	10.700	0.013	0.748	0.015	0.204	0.015	10.687	0.700	0.196
LHS1967	13.472	0.022	0.704	0.024	0.229	0.041	13.460	0.659	0.220
LHS1995	13.551	0.076	0.340	0.078	0.138	0.079	13.545	0.318	0.133
LHS1996	11.791	0.014	0.703	0.019	0.162	0.015	11.778	0.658	0.156
LHS2011	8.689	0.013	0.717	0.018	0.201	0.014	8.677	0.671	0.193
LHS2012	14.129	0.070	0.577	0.085	0.209	0.089	14.119	0.540	0.201
LHS2039	11.022	0.011	0.995	0.019	0.439	0.019	11.004	0.931	0.421
LHS2056	9.208	0.012	0.526	0.014	0.095	0.012	9.199	0.492	0.092
LHS2059	11.882	0.009	0.666	0.014	0.148	0.014	11.870	0.623	0.142
LHS2066	11.093	0.009	0.689	0.012	0.115	0.011	11.081	0.645	0.110
LHS2081	8.043	0.012	0.850	0.013	0.162	0.015	8.028	0.795	0.155
LHS2095	10.101	0.010	0.612	0.014	0.100	0.011	10.089	0.573	0.096
LHS2115	12.630	0.012	0.777	0.022	0.303	0.018	12.617	0.727	0.291
LHS2161	8.733	0.013	0.717	0.015	0.094	0.019	8.721	0.671	0.091
LHS2224	8.500	0.011	0.792	0.011	0.294	0.012	8.486	0.741	0.282
LHS2225	10.698	0.008	0.803	0.011	0.254	0.010	10.683	0.751	0.243
LHS2229	14.565	0.062	0.479	0.068	0.200	0.107	14.556	0.449	0.192
LHS2243	10.923	0.017	1.068	0.021	1.177	0.023	10.903	1.000	1.130
LHS2250	12.656	0.037	0.744	0.040	0.185	0.044	12.643	0.697	0.178
LHS2284	9.957	0.007	0.610	0.010	0.079	0.009	9.946	0.571	0.076
LHS2290	10.759	0.007	0.750	0.010	0.250	0.011	10.746	0.702	0.240
LHS2312	11.098	0.020	0.747	0.027	0.162	0.028	11.085	0.699	0.156
LHS2330	11.479	0.013	0.960	0.020	0.371	0.017	11.461	0.898	0.356
LHS2340	10.107	0.009	0.258	0.012	0.028	0.011	10.102	0.241	0.027
LHS2341	13.104	0.052	0.715	0.055	0.354	0.059	13.091	0.669	0.340
LHS2342	11.957	0.023	0.789	0.028	0.323	0.026	11.943	0.739	0.311
LHS2345	10.468	0.011	0.946	0.011	0.381	0.014	10.450	0.886	0.366
LHS2349	11.416	0.021	0.743	0.024	0.203	0.023	11.402	0.695	0.195
LHS2351	11.320	0.010	1.010	0.010	0.390	0.000	11.300	0.940	0.380
LHS2352	14.750	0.060	0.760	0.080	0.330	0.040	14.730	0.710	0.320
LHS2415	7.701	0.009	0.793	0.010	0.276	0.009	7.687	0.742	0.265
LHS2421	11.548	0.008	0.735	0.014	0.216	0.011	11.535	0.688	0.207
LHS2424	9.654	0.015	0.461	0.016	0.059	0.016	9.646	0.431	0.056
LHS2431	10.136	0.011	0.776	0.013	0.230	0.012	10.122	0.726	0.220
LHS2440	10.657	0.021	0.652	0.022	0.830	0.025	10.645	0.610	0.797
LHS2449	11.219	0.019	0.728	0.023	0.209	0.021	11.206	0.681	0.201
LHS2450	8.962	0.008	0.346	0.009	0.039	0.009	8.955	0.324	0.038
LHS2461	9.264	0.010	0.887	0.013	0.300	0.010	9.249	0.830	0.288
LHS2463	9.801	0.009	0.684	0.011	0.144	0.010	9.789	0.641	0.138
LHS2467	9.775	0.007	0.651	0.009	0.127	0.010	9.763	0.609	0.122
LHS2483	11.416	0.014	0.833	0.016	0.323	0.023	11.401	0.780	0.310

TABLE 2. (continued)

Star	UKIRT System						CIT System			oł
	K	σ	$(J-K)$	$\sigma J-K$	$(H-K)$	$\sigma H-K$	K	$(J-K)$	$(H-K)$	
LHS2626	11.550	0.010	0.750	0.020	0.250	0.000	11.540	0.700	0.240	M
LHS2627	13.020	0.030	0.720	0.040	0.220	0.000	13.010	0.680	0.210	M
LHS2632	11.210	0.020					11.200			J
LHS2666	9.510	0.010	0.780	0.030			9.500	0.730		M
LHS2679	12.750	0.020	0.720	0.030	0.220	0.000	12.730	0.670	0.210	M
LHS2694	12.430	0.010	0.730	0.020	0.220	0.000	12.420	0.680	0.210	M
LHS2708	10.180	0.000	0.640	0.010	0.110	0.000	10.170	0.600	0.110	M
LHS2720	12.130	0.030	0.730	0.030	0.220	0.000	12.120	0.690	0.210	M
LHS2723	14.180	0.060	0.550	0.060	0.180	0.000	14.180	0.520	0.180	M
LHS2753	12.560	0.020	0.690	0.050	0.260	0.050	12.550	0.650	0.260	J
LHS2765	9.690	0.010	0.580	0.020	0.120	0.000	9.670	0.540	0.120	M
LHS2818	14.31	0.040					14.300			J
LHS2823	14.000	0.020	0.650	0.020	0.190	0.000	13.990	0.610	0.180	M
LHS2824	9.760	0.020					9.750			J
LHS2831	9.950	0.010	0.890	0.010	0.340	0.000	9.930	0.830	0.330	M
LHS2832	10.640	0.000	0.770	0.010	0.160	0.000	10.630	0.720	0.150	M
LHS2838	11.540	0.010	0.890	0.010	0.300	0.000	11.520	0.840	0.290	M
LHS2851	12.630	0.010	0.730	0.010	0.190	0.000	12.620	0.690	0.180	M
LHS2864	9.030	0.020	0.780	0.030			9.020	0.730		J
LHS2873	10.170	0.010	0.670	0.010	0.100	0.000	10.160	0.630	0.100	M
LHS2874	12.430	0.010	0.740	0.020	0.190	0.000	12.420	0.700	0.180	M
LHS2901	12.150	0.010	0.700	0.010	0.160	0.000	12.140	0.650	0.150	M
LHS2902	11.930	0.020	0.680	0.020	0.180	0.000	11.920	0.640	0.170	M
LHS2946	9.750	0.020					9.740			J
LHS2951	15.600	0.110	0.180	0.120	0.070	0.000	15.590	0.170	0.060	M
LHS2954	10.460	0.020	0.820	0.030	0.280	0.010	10.450	0.770	0.270	J
LHS2968	8.750	0.010	0.490	0.010			8.740	0.450		M
LHS2980	11.430	0.020	0.980	0.030	0.350	0.020	11.41	0.920	0.330	J
LHS3009	8.660	0.010	0.890	0.010	0.310	0.000	8.650	0.830	0.300	M
LHS3010	12.280	0.030	0.170	0.030	0.320	0.000	12.280	0.160	0.310	M
LHS3019	13.940	0.050	0.760	0.060	0.230	0.010	13.920	0.710	0.220	J
LHS3034	10.280	0.010	0.470	0.030	0.050	0.000	10.270	0.440	0.050	M
LHS3041	12.030	0.010	0.750	0.020	0.190	0.000	12.020	0.700	0.180	M
LHS3073	10.390	0.020	0.710	0.020	0.170	0.000	10.380	0.670	0.160	M
LHS3082	12.940	0.020	0.700	0.030	0.150	0.030	12.930	0.650	0.150	J
LHS3085	13.860	0.030	0.690	0.060	0.240	0.050	13.850	0.650	0.230	J
LHS3090	13.910	0.030	0.550	0.040	0.160	0.030	12.930	0.650	0.260	J
LHS3094	12.260	0.020					12.250			J
LHS3098	13.230	0.040	0.740	0.040	0.240	0.000	13.220	0.700	0.230	M
LHS3101	11.350	0.000	0.730	0.010	0.180	0.000	11.330	0.680	0.170	M
LHS3102	12.870	0.010	0.710	0.020	0.200	0.000	12.850	0.670	0.190	M
LHS3113	11.720	0.010	0.770	0.010	0.250	0.000	11.700	0.720	0.240	M
LHS3121	11.550	0.010	0.870	0.010	0.290	0.000	11.540	0.820	0.270	M
LHS3125	14.150	0.060	0.550	0.060	0.220	0.000	14.140	0.520	0.210	M
LHS3170	14.180	0.020					14.170			J
LHS3177	9.990	0.010	0.820	0.020	0.310	0.000	9.980	0.760	0.300	M
LHS3189	12.690	0.030	0.750	0.030	0.270	0.000	12.680	0.700	0.260	M
LHS3263	14.110	0.020	0.680	0.040	0.210	0.000	14.100	0.640	0.200	M
LHS3276	11.340	0.020	0.720	0.020	0.190	0.000	11.330	0.670	0.180	M

TABLE 2. (continued)

Star	UKIRT System						CIT System			
	K	σ	$(J-K)$	$\sigma J-K$	$(H-K)$	$\sigma H-K$	K	$(J-K)$	$(H-K)$	o
LHS3455	11.570	0.020	0.810	0.020	0.320	0.000	11.560	0.750	0.310	M
LHS3493	9.940	0.010	0.780	0.020	0.210	0.000	9.930	0.730	0.200	M
LHS3579	11.420	0.020	0.580	0.030	0.080	0.000	11.410	0.550	0.080	M
LHS3599	9.160	0.020					9.150			:
LHS3633	10.380	0.030					10.370			:
LHS3733	11.690	0.020	0.680	0.030	0.100	0.010	11.670	0.640	0.100	:
LHS3783	8.470	0.000			0.940	0.000	8.700		0.900	M
LHS3845	10.760	0.030	0.840	0.030	0.230	0.020	10.750	0.780	0.220	:
LHS3867	10.570	0.013	0.637	0.016	0.162	0.020	10.559	0.596	0.156	Γ
LHS3868	14.420	0.030	0.710	0.030	0.120	0.020	14.400	0.670	0.120	:
LHS3950	11.370	0.045	0.773	0.045	0.268	0.046	11.356	0.724	0.257	Γ
LHS3961	12.531	0.044	0.558	0.047	0.086	0.048	12.521	0.522	0.083	Γ
LHS3962	10.051	0.029	0.827	0.032	0.285	0.029	10.036	0.774	0.274	Γ
LHS4017	11.389	0.013	0.746	0.014	0.260	0.016	11.376	0.698	0.250	Γ
LP381-86	12.960	0.030	0.710	0.040	0.210	0.000	12.950	0.670	0.200	M
DL CAS	5.996	0.007	0.635	0.010	0.206	0.007	5.984	0.594	0.198	Γ
G17-16	10.520	0.020	0.730	0.040	0.230	0.000	10.510	0.690	0.230	M
G111-33	7.800	0.010	0.386	0.012	0.073	0.012	7.793	0.361	0.070	Γ
G112-1	12.666	0.037	0.445	0.039	0.098	0.037	12.658	0.416	0.094	Γ
G121-58	10.370	0.010	0.770	0.010	0.200	0.000	10.350	0.720	0.190	M
G166-37	10.790	0.010	0.420	0.020	0.060	0.000	10.780	0.390	0.050	M
G233-27	11.988	0.017	0.728	0.027	0.180	0.029	11.975	0.682	0.173	Γ

and the average scatter in the transformation of an individual standard star observation to the standard system was: $\sigma(K) = 0.013$ mag; $\sigma(J - K) = 0.023$ mag; $\sigma(H - K) = 0.019$ mag. Given the uncertainties in the standard star values themselves, the scatter in our transformations is excellent. During the shorter nights of May 1995 we observed from 6 to 8 standards per night. The more humid weather led to reduced precision in the photometry, with $\sigma(K) = 0.030$ mag, $\sigma(J - K) = 0.024$ mag, and $\sigma(H - K) = 0.033$ mag. The June 1995 observing run proved difficult. The weather was acceptable for half or all of 3 nights, but COB experienced intermittent cable connection failures, leading to occasional variable background noise levels. All of the frames in which variable background was discerned were discarded, but fewer measures of standard stars were thereby available for analysis. Rather than deriving the slopes of the $J - K$, $J - H$, and $H - K$ transformations independently, we adopted the mean values from the previous month's observing (which were also consistent, as we have noted, with the December 1994 observing). We solved only for zero points in the transformations. The total number of standards available was reduced to between 4 and 6 for each of the three nights. The smaller number of standards, the higher humidity, and the residual background problems combined to yield poorer photometry, with mean values of $\sigma(K) = 0.045$ mag, $\sigma(J - K) = 0.047$ mag, and $\sigma(H - K) = 0.053$ mag.

III. JHK PHOTOMETRY

The final step involved transformation of the UKIRT photometric system results into the "CIT" system (Elias *et al.* ., 1982), using the transformations provided by Casali & Hawarden (1992). These transformations are:

$$K_{CIT} = K_{UKIRT} - 0.018 \times (J - K) \tag{1}$$

$$(J - K)_{CIT} = 0.936 \times (J - K)_{UKIRT} \tag{2}$$

$$(H - K)_{CIT} = 0.960 \times (H - K)_{UKIRT}. \tag{3}$$

In Table 2. we summarize the results for the program stars. The errors quoted represent the combination of the measurement errors (determined from the multiple measures) and the errors involved in the transformations to the standard systems. The latter are important only for the data obtained during June of 1995. The Table also identifies during which observing run the data were taken (December 1994 = D94; May 1995 = M95; June 1995 = J95).

IV. SUMMARY

The program stars of field population II candidates were selected by the reduced proper motion diagram among the stars in the LHS catalogue class k and m. JHK photometric observations were made by the COB equipped to the Kitt Peak telescopes. JHK photometry for two hundred two stars are presented.

ACKNOWLEDGEMEMT

REFERENCES

Bahcall, J., & Casertano, S. 1986, ApJ, 308, 347
Bahcall, J., Flynn, C., Gould, A., & Kirhakos, S. 1995, ApJ, 435, L51
Casali, M., & Hawarden, T. 1992, *The JCMT - UKIRT Newsletter No. 4*
Dahn, C., Liebert, J., Harris, H., & Guetter, H. C. 1995, in *An ESO Workshop on: The Bottom of the Main Sequence and Beyond, ed. C. G. Tinny*
Dawson, P. C. 1986, ApJ, 311, 984

Eggen, O. J. 1983, ApJS, 51, 183

———- 1987, AJ, 93, 393

Elias, 1982, AJ, 97, 1029

Elson, R. A. W., Santiago, B. X., & Gilmore, G. F. 1996, New Astronomy in press

Giclas, H., Burnham, R., & Thomas, N. 1968, Lowell Obs. Bull. No. 7, 67

Kroupa, P., & Tout, C. A. 1997, MN in press

Lee, S.-G. 1985, JKAS, 18, 70

———- 1991, JKAS, 24, 161

———- 1993, JKAS, 26, 141

———- 1995, JKAS, 28, 139

Luyten, W. 1976, *LHSCatalogue*, University of Minnesota

Mendez, R. A., Minniti, D., de Marchi, G., Baker, A., & Couch, W. J. 1996, MN, in press

Reid, N., & Majewski, S. R. 1993, ApJ, 409, 635

Richer, H. B., & Fahlman, G. G. 1992, Nature, 358, 353

Schmidt, M. 1975, ApJ, 202, 22

Stetson, P. B. 1987, PASP, 99, 191

———— 1990, PASP, 102, 932

Tucker, K. D., Dickman, R. L., Encrenaz, P. J.,& Kutner, M. L. 1976, ApJ, 210, 679